A Modular Low Current Ripple Electrolysis Power Supply Based on Multiphase Half-Bridge High-Frequency Inverters

Huagen Xiao

***Abstract*—This article presents a modular low current ripple electrolysis power supply topology based on multiphase high-frequency inverter and its control method. The topology of the electrolysis power supply consists of ac–dc converter and dc–dc converter. Among them, the dc–dc converter is composed of a plurality of modular small-capacity dc–dc conversion modules connected in parallel. Each dc–dc conversion module is composed of a half-bridge high-frequency inverter and a full-wave rectifier. By controlling the output voltage of the high-frequency inverter in each dc–dc conversion module and staggering the equal phase angle in sequence, the low-frequency harmonic components in the dc voltage at the output terminals of multiple dc–dc conversion modules are eliminated. Finally, simulation and experimental results show that the proposed electrolysis power supply can provide low ripple current for the load, which provides technical guarantee for the production of high-quality electrolytic copper foil.**

***Index Terms*—AC–DC power converters, current control, dc–ac power converters, dc–dc power converters.**

I. Introduction

ELECTROLYSIS power supply is widely used in electrolysis, electroplating, electrophoresis, electrochemistry, and other industries, and its current or voltage ripple coefficient is directly related to the quality of related products. It is important to study the low-voltage high-current electrolysis power supply with low voltage ripple to improve the quality of electrolytic copper foil and electroplating effect [1]–[4].

The low-voltage high-current electrolysis power supply is usually composed of front-stage ac–dc rectifier and poststage dc–dc converter. Because the three-phase voltage-type pulsewidth modulation (PWM) rectifier has the advantages of good sinusoidal input current, high power factor, and four-quadrant operation, which can overcome the disadvantages of large input current harmonics and low power factor in the conventional uncontrollable rectifier circuit. Three-phase voltage-type PWM rectifiers have become the main topology of front-stage ac–dc rectifier in modern electrolysis power supplies [5], [6]. Different application fields have different technical specifications for the output voltage and current of the dc–dc converter, so the poststage dc–dc converter is still a research hotspot for electrolysis power supply [7]–[10].

At present, the technologies aim to eliminate the ripple components in the output voltage or output current of low-voltage high-current switching power supply mainly include increasing the pulse wave number of the three-phase ac input voltage of the front-stage ac–dc converter, the multiple parallel connection of the secondary winding of the high-frequency transformer in the poststage dc–dc converter, and the output voltage frequency of the high-frequency inverter [11]–[19]. In order to increase the pulse wave number of the three-phase ac input voltage of the front-stage ac–dc converter, Buddingh and Mars [11] and Agalgaonkar *et al*. [13] proposed that multiple transformers with different primary winding connection modes are connected to the rectifier. The solution effectively reduces the harmonic current in the input current of the ac side, but the hardware cost of the solution is high and the architecture is complicated. In order to implement the multiple connections of the secondary winding of high-frequency transformers, Solanki *et al*. [14] and Saleh *et al*. [15] proposed a medium-voltage switching power supply based on modular multilevel mid-frequency inverter. The proposed architecture has the advantages of high efficiency, high input power factor, and high power quality, but the number of power electronic devices is large, and the independence of the dc–dc module is not good. In [16], a synchronous rectifier based on MOSFET is proposed, which can effectively reduce the output voltage ripple by controlling the switching action of MOSFET in the synchronous rectifier connected to the secondary side of the transformer, but the control method is complicated. Coulinge *et al.* [17] put forward the low-voltage high-current Large Hadron Collider power supply based on the transformer with the primary winding connected in series and the secondary winding connected in parallel. The inverter and transformer do not have the advantage of modular architecture solution.

In order to eliminate the output voltage ripple of the dc–dc converters, a three-phase zero voltage switching dc–dc converter associated with a positive double-star active rectifier and a reduced current unbalance transformer for high-power-density energy conversion are proposed for server power supply in

Manuscript received January 14, 2020; accepted February 24, 2020. Date of publication March 5, 2020; date of current version June 23, 2020. This work was supported in part by the Hunan Provincial Natural Science Foundation of China under Grant 2017JJ2085, in part by the Scientific Research Fund of Hunan Provincial Education Department under Grant 17C0637, and in part by China Postdoctoral Science Foundation under Project 2018M643800XB. Recommended for publication by Associate Editor D. M. Xu.

The author is with the School of Information and Electrical Engineering, Hunan University of Science and Technology, Xiangtan 411201, China (e-mail: xiaohuagen@163.com).

Color versions of one or more of the figures in this article are available online at http://ieeexplore.ieee.org.

Digital Object Identifier 10.1109/TPEL.2020.2978340

[18], in which the rectifier is composed of six power electronic devices (MOSFETs) at the low-side of the rectifier transformer. The proposed architecture can effectively reduce the voltage stress on the power electronic device and the output voltage ripple of the switching power supply. However, a large number of electronic devices and a five-legged rectifier transformer need to be added. In [19], different types of modular rectifier and the output voltage phase interleaving control method of inverters are proposed, and the proposed power supply modules are independent and the output voltage ripple of the dc–dc converter is small. However, since each module uses an independent front-stage ac–dc rectifier, the input voltage ripple of each dc–dc converter module is inconsistent with each other, which may result in uneven output voltage ripple in the dc–dc converter modules [20], [21]. At the same time, the ac-side voltage of the ac–dc rectifier is relatively high, and the hardware cost is high when each module adopts the independent high-voltage low-power rectification circuit.

This article presents a low current ripple modular electrolysis power supply topology based on multiphase half-bridge high-frequency inverter and automatic phase equalization staggered control method. In the proposed topology of the electrolysis power supply, the front-stage PWM rectifier provides a uniform dc voltage for the poststage modular dc–dc converters, and each dc–dc conversion module is composed of a half-bridge high-frequency inverter, a center-tapped high-frequency transformer, and a full-wave uncontrollable rectifier. The proposed control method includes the automatic phase equalization staggered control method and the virtual resistance current-sharing control algorithm based on the current sharing deviation. The advantages of the proposed topology and control method are as follows.

1) The poststage modular dc–dc converter is powered by the same dc voltage, which can prevent the influence of the input dc voltage ripple on the accuracy of the phase equalization staggered control of the poststage dc–dc conversion modules.
2) The use of a half-bridge high-frequency inverter in a dc–dc conversion module can reduce the voltage stress on following stage circuit.
3) The automatic phase equalization staggered control enables the free parallel connection of the poststage dc–dc modules and reduces the total output current ripple of the dc–dc conversion modules.
4) The virtual resistance current-sharing control algorithm based on the current-sharing deviation can realize the automatic equalization of the output current of each dc–dc conversion module connected in parallel. In view of the aforementioned analysis, the proposed electrolysis power supply topology and control method can facilitate system hardware maintenance, reduce current ripple, and flexibly control multiple dc–dc parallel modules.

This article is organized as follows. In Section II, the topology of low current ripple electrolysis power supply is proposed, and the theoretical feasibility of current ripple suppression is analyzed. The automatic phase equalization staggered control for the modular electrolysis power supply is presented in Section III. The simulation and experimental results are given in Section IV. Finally, Section V concludes this article.

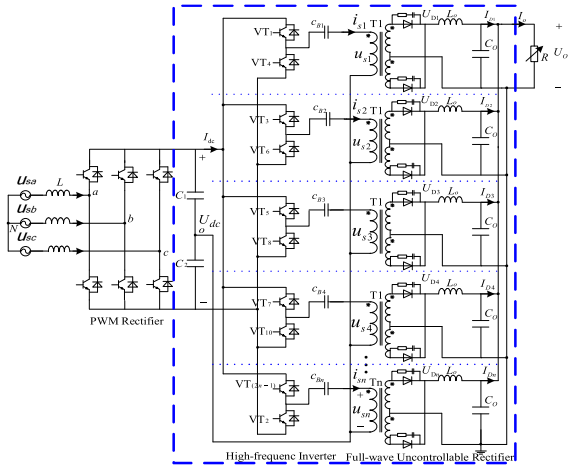

Fig. 1. Topological structure of electrolysis power supply.

II. Topology and Current Ripple Analysis of Electrolysis Power Supply

A. Topology and Working Principle

The topological structure of electrolysis power supply is shown in Fig. 1, including PWM rectifier and dc–dc converter.

The modular structure has become a trend in high-current dc–dc converters. Therefore, this article proposes a modular dc–dc conversion, as shown in the dotted line of Fig. 1, and the dc–dc conversion circuit is composed of n dc–dc conversion modules. The input and output end of each dc–dc converter module is connected in parallel, respectively. Each dc–dc conversion module consists of a high-frequency inverter, a center-tapped high-frequency transformer, and a full-wave uncontrollable rectifier. At the same time, the phases of the output voltages of each high-frequency inverters are evenly interleaved by the control algorithm, which can reduce the total output current ripple of the electrolysis power supply. First, the three-phase ac voltage of the distribution grid is regulated by the PWM rectifier to obtain $U_{\rm dc}$, and n sets of single-phase half-bridge inverters are used to obtain n-phase equal phase-shifted high-frequency ac voltage $u_{sx(x=1,2,\ldots,n)}$. Then, I_{Dn} is obtained by the full-wave rectifier, and I_{Dn} are connected in parallel to obtain I_o.

From Fig. 1, it can be seen that the proposed topology has less insulated gate bipolar transistor (IGBT) or MOSFET than paralleling multiple dual active bridges (DABs), the comparison results are shown in Table I.

As can be seen from Table I, in similar low-voltage high-current power supply systems, the dc–dc topology proposed in this article requires the minimum number of switching devices, which will have a cost advantage. As for the electrolytic power supply, the poststage dc–dc does not need bidirectional energy control, so the control system is simpler than DAB structure. However, the large number of MOSFETs drivers are difficultly in

TABLE I
NUMBER OF SWITCHING DEVICES IN DIFFERENT TOPOLOGIES

Device names in different topologies	Topology proposed in [3]	Topology proposed in [10]	Topology proposed in [19]	The topology of DAB	Topology proposed in this paper
Number of IGBT and MOSFET	4	4	4	8	2
Number of diode	2	2	2	0	2
Number of Transformer	1	1	1	1	1

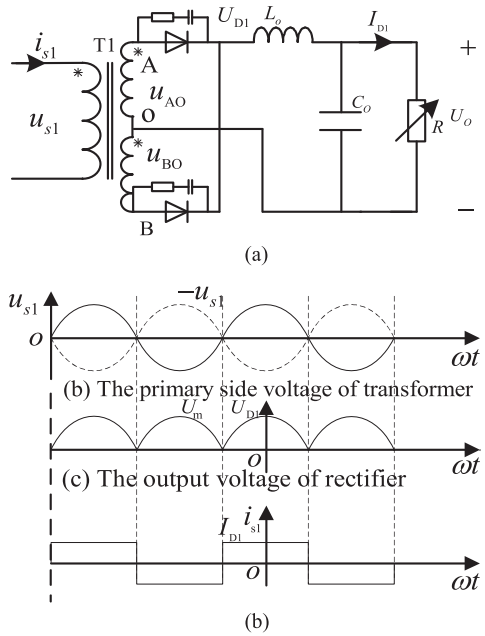

Fig. 2. Schematic and waveform of full wave rectifier with center tapped transformer.

consistent with each other when the paralleling multiple DABs are adopted in high-current electrolytic power.

B. Current Ripple Analysis

Fig. 2 shows the relevant parameters of the full-wave uncontrollable rectifier. The load of the electrolysis power supply is a low-resistance electrolyte containing metal ions. In order to increase the smoothness of the output current of the electrolysis power supply, the inductance value of the output filter is usually large. Therefore, the dc-side load of a full-wave uncontrollable rectifier can be considered as a pure inductor, and the dc-side load current is approximately a constant dc [20].

Take a set of full-wave uncontrollable rectifier as an example, u_{s1} is controlled to be a sinusoidal ac voltage $U_m \sin \omega t$, and the input alternating current $i_{s1}(t)$ is a 180° square wave, as shown in Fig. 2(d), with a period of 2π. If the zero point of the time coordinate is taken at the peak time of the sine wave, as shown in Fig. 2, the expression of u_{s1} is $U_m \cos \omega t$, and then the expression of the Fourier series of $i_{s1}(t)$ is as follows:

$$i_{s1}(t)=\frac{4}{\pi}I_{D1}\left\{\begin{array}{l}\cos\omega t-\frac{1}{3}\cos 3\omega t+\frac{1}{5}\cos 5\omega t-\frac{1}{7}\cos 7\omega t+\\ \frac{1}{9}\cos 9\omega t-\frac{1}{11}\cos 11\omega t+\frac{1}{13}\cos 13\omega t\cdots\end{array}\right\}. \tag{1}$$

If the power conversion loss of the transformer is ignored, according to the working principle of the transformer, we can obtain

$$u_{s1}\cdot i_{s1}=U_{D1}\cdot I_{D1}. \tag{2}$$

Then

$$U_{D1}=\frac{u_{s1}\cdot i_{s1}}{I_{D1}}=\frac{4}{\pi}U_m\left\{\begin{array}{l}\frac{1}{2}+\frac{1}{1\times 3}\cos 2\omega t-\frac{1}{3\times 5}\cos 4\omega t+\\ \frac{1}{5\times 7}\cos 6\omega t-\frac{1}{7\times 9}\cos 8\omega t+\cdots\end{array}\right\}. \tag{3}$$

It can be seen that the harmonic component in U_{D1} is dominated by the double frequency component from (3).

When $n=2$, we control u_{s1} and u_{s2} to be as following:

$$\left\{\begin{array}{l}u_{s1}=\sin(\omega t)\\ u_{s2}=\sin\left(\omega t-\frac{2\pi}{2}\right).\end{array}\right. \tag{4}$$

Then

$$\frac{U_o}{R}\approx\frac{U_{D1}-U_o}{sL_o}+\frac{U_{D2}-U_o}{sL_o}. \tag{5}$$

That is

$$U_o=\frac{U_{D1}+U_{D2}}{\frac{sL_o}{R}+2}. \tag{6}$$

Let $k=1/(\frac{sL_o}{R}+2)$, there is

$$U_o=k\cdot\frac{4}{\pi}U_m\left\{\begin{array}{l}1+\frac{2}{1\times 3}\cos 2\omega t-\frac{2}{3\times 5}\cos 4\omega t+\\ \frac{2}{5\times 7}\cos 6\omega t-\frac{2}{7\times 9}\cos 8\omega t+\cdots\end{array}\right\}. \tag{7}$$

When $n=3$, we control u_{s1}, u_{s2}, and u_{s3} to be as following, respectively:

$$\left\{\begin{array}{l}u_{s1}=\sin(\omega t)\\ u_{s2}=\sin\left(\omega t-\frac{2\pi}{3}\right)\\ u_{s3}=\sin\left(\omega t-\frac{4\pi}{3}\right).\end{array}\right. \tag{8}$$

Similarly, the Fourier series expressions for $i_{s2}(t)$ and $i_{s3}(t)$ are

$$i_{s2}(t)=\frac{4}{\pi}I_{D1}\left\{\begin{array}{l}\cos\left(\omega t-\frac{\pi}{3}\right)-\frac{1}{3}\cos 3\left(\omega t-\frac{\pi}{3}\right)+\\ \frac{1}{5}\cos 5\left(\omega t-\frac{\pi}{3}\right)-\frac{1}{7}\cos 7\left(\omega t-\frac{\pi}{3}\right)+\cdots\end{array}\right\} \tag{9}$$

$$i_{s3}(t)=\frac{4}{\pi}I_{D1}\left\{\begin{array}{l}\cos\left(\omega t-\frac{2\pi}{3}\right)-\frac{1}{3}\cos 3\left(\omega t-\frac{2\pi}{3}\right)+\\ \frac{1}{5}\cos 5\left(\omega t-\frac{2\pi}{3}\right)-\cdots\end{array}\right\}. \tag{10}$$

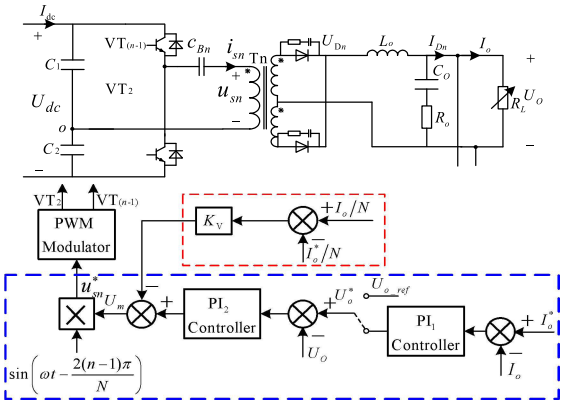

Fig. 3. Schematic diagram of the *n*th dc–dc conversion module and its output current control.

Then

$$U_o = k \cdot (U_{D1} + U_{D2} + U_{D3}) = k \cdot \frac{4}{\pi} U_m \left\{ \frac{3}{2} + \frac{3}{5 \times 7} \cos 6\omega t + \frac{3}{11 \times 13} \cos 12\omega t - \cdots \right\} \tag{11}$$

where $k = 1/(\frac{sL_o}{R} + 3)$.

Additionally, when N(N is odd) sets of full-wave uncontrollable rectifiers with the center-tapped transformer is connected in parallel to build an electrolysis power supply, the output voltage of the *n*th high-frequency inverter is

$$u_{sn} = U_m \sin\left(\omega t - \frac{2(n-1)\pi}{N}\right). \tag{12}$$

Then, the dc voltage of the electrolysis power supply can be expressed as following:

$$U_o = \frac{4k}{\pi} U_m \left\{ \begin{array}{l} \frac{N}{2} + (-1)^{(N-1)} \frac{N}{(2N-1)\times(2N+1)} \cos 2N\omega t + \\ (-1)^{(N-1)} \frac{N}{(4N-1)\times(4N+1)} \cos 4N\omega t + \cdots \end{array} \right\} \tag{13}$$

where $k = 1/(\frac{sL_o}{R} + N)$.

By comparing (3), (11), and (13), if the phase angle of the output voltage of each high-frequency inverter is controlled to be evenly displaced, the low-frequency harmonic components in the output voltage of the full-wave uncontrollable rectifier can be eliminated. Then, the output voltage ripple of the electrolysis power supply can be effectively eliminated.

III. Low Current Ripple Control Method for DC–DC Conversion Modules

From Fig. 3, it can be seen that the dc–dc converter proposed in this article consists of multiphase high-frequency inverter, high-frequency isolation transformer, and full-wave rectifier. Among them, the phase angles of the output voltage reference value of each high-frequency inverter are evenly interleaved, and the control method for the output current of each dc–dc conversion module is the same. The single dc–dc conversion module and its output current control principle in the low current ripple electrolysis power supply with N sets of dc–dc conversion modules are shown in Fig. 3. In Fig. 3, the content in the blue dotted frame is the automatic phase equalization staggered control method, and the content in the red dotted frame is the current-sharing deviation based virtual resistance current-sharing control algorithm embedded in the automatic phase equalization staggered controller. The split dc-link with series cap is good for voltage stress reduction on following stage, but there is voltage imbalance problem under high load conditions, which may worsen the parallel conditions. Therefore, the virtual resistance current-sharing control algorithm is used to achieve the automatic equalization of the output current of each dc–dc conversion module connected in parallel. In particular, the topology and control method proposed in this article are applicable to both constant current and constant voltage modes, and the rest of this article is only for the current source operating mode. For the production process requiring a constant voltage, it is only necessary to switch the input reference value of the voltage control loop to the output voltage reference value in Fig. 3. In Fig. 3, n is the serial number of the high-frequency inverter, and K_V is the virtual impedance based current-sharing deviation [23].

The relationship between the output current and the load of the dc–dc converter module is $I_o = U_o/R_L$. Because the load is randomly changed, and electrolysis, electroplating, and other processes require constant current, the output voltage of the dc–dc conversion module should be adjusted accordingly with changes in the load resistance. In order to adapt to the random changes in the load, the first PI controller is used to achieve precise control of the output current of the dc–dc conversion module. That is

$$U_o^* = \left(k_{p1} + \frac{k_{i1}}{S}\right)(I_o^* - I_o). \tag{14}$$

The relationship between the output voltage of the dc–dc conversion module and the dc-side voltage of the front-stage PWM rectifier is as follows:

$$U_o = k_{\mathrm{T}n} \times D \times \frac{U_{dc}}{2} \tag{15}$$

where $k_{\mathrm{T}n}$ and D is the transformation ratio of high-frequency transformer and the On-duty ratio of the power switching devices of the high-frequency inverter, respectively.

It can be seen that the output voltage of the dc–dc conversion module can be controlled by controlling the On-duty ratio of the power switching devices in the upper and lower bridge arms of the high-frequency inverter. The second PI controller is used to control the output voltage amplitude of the high-frequency inverter in the dc–dc conversion module. The automatic phase equalization staggered control is achieved by giving a sine function that automatically sets the equal phase shift angle according to (12) and the number of dc–dc conversion modules connected in parallel. So, there is

$$\left\{ \begin{array}{l} U_m = \left(k_{p2} + \frac{k_{i2}}{S}\right)(U_o^* - U_o) \\ u_{sn} = U_m \sin\left(\omega t - \frac{2(n-1)\pi}{N}\right). \end{array} \right. \tag{16}$$

When the transformation ratio of the high-frequency isolation transformer is 1:1:1, the dc component of the output voltage

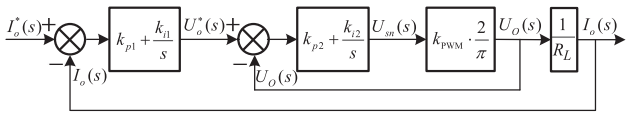

Fig. 4. Schematic diagram of the control system for a single dc–dc module.

of the dc–dc conversion module can be obtained from (13) as following:

$$U_o \approx \frac{2}{\pi} U_m. \tag{17}$$

Therefore, the diagram of the control system of a single dc–dc conversion module is shown in Fig. 4.

According to the Rolls stability criterion and the control system index requirements, the proportional integral coefficients of the inner and outer loop controllers can be obtained, respectively, [24].

IV. Simulation and Experimental Analysis

In order to verify the effectiveness of the topology and control method of the low voltage ripple electrolysis power supply proposed in this article, the power supply model shown in Fig. 1 was built in the simulation software PSIM9 and a 1-kW prototype of electrolysis power supply was built in the laboratory. The main parameters of the electrolysis power supply are as follows. The three-phase ac input voltage of the front-stage PWM rectifier is 380 V, and the rated voltage of the dc-side capacitor of the PWM rectifier is 660 V. The switching frequency of the front-stage PWM rectifier is 10 kHz, the switching frequency of the poststage multiphase high-frequency inverter is 100 kHz, and the fundamental frequency of the ac output voltage of the high-frequency inverter is 1 kHz. The blocking capacitor C_{Bn} is connected in series with the high-frequency transformer to eliminate any low-frequency component of the magnetizing current that may increase the flux density of the transformer. At the same time, in order to reduce the voltage loss on the blocking capacitor, the value of C_{Bn} is mainly based on the primary-side inductance value and voltage frequency of the high-frequency transformer ($C_{Bn}$is 250 μF). At the same time, a resistor R_o whose resistance is much larger than the load resistance value is connected in series with the output filter capacitor C_o to suppress C_o from generating an inrush current to the load. The ratio of high-frequency transformer (T_n) is 1:1:1, $L_o$is 1 mH, and $C_o$is 600 μF, and R_o is 1 Ω. The circuit parameters of the low current ripple electrolysis power supply are listed in Table II.

TABLE II
Circuit Parameters of the Low Voltage Ripple Electrolysis Power Supply

Parameters	Value
Ratio of High-frequency Transformer T_n	1:1:1
Switching Frequency of PWM Rectifier $f_{\rm PWM1}$	10 kHz
Switching Frequency of High-frequency Inverter $f_{\rm PWM2}$	100 kHz
Output Voltage Frequency of High-frequency Inverter $f_{\rm INV}$	1 kHz
Output Filter Inductance $L_{\rm o}$	1 mH
Blocking Capacitor C_{Bn}	250 uF
Output Filter Capacitor C_o	600 uF
Impulse Current Damping Resistor R_o	1 Ohm

A. Simulation

1) Simulation Scheme 1: In the simulation scheme, the rated output current of the poststage dc–dc converter is 1 kA, and a pure resistance of 0.008 Ω is used to simulate the load of the electrolysis power source. In order to verify that the dc output current of the electrolysis power supply adopting the topology and control method proposed in this article has the above-mentioned theoretical analysis effect in improving the ripple, Fig. 5 shows the simulation results of the electrolysis power supplies using different dc–dc converter topology and corresponding control methods.

Fig. 5(a) shows the simulation result of a single dc–dc converter module and Fig. 5(b) shows the simulation results when the electrolysis power supply based on the parallel configuration of three dc–dc converter modules is applied with the control method proposed in this article. Fig. 5(c) is the simulation result when the electrolysis power supply based on the parallel configuration of five dc–dc converter modules is applied with the control method proposed herein.

In Fig. 5, $U_{\rm dc}$ is the dc-side capacitor voltage of prestage PWM rectifier. $I_{\rm o1}$ is the dc output current of a single dc–dc converter module, $I_{\rm o3-new}$ is the dc output current of three dc–dc converter modules connected in parallel, and $I_{\rm o5-new}$ is the dc output current of five dc–dc converter modules connected in parallel. $I_{\rm dc1}$ is the dc input current of a single dc–dc converter module, $I_{\rm dc3-new}$ is the dc input current of three dc–dc converter modules connected in parallel, and $I_{\rm dc5-new}$ is the dc input current of five dc–dc converter modules connected in parallel. It can be seen from Fig. 5 that the output current ripple characteristic of the electrolysis power supply used the topology and control method proposed in this article is better than that of a single dc–dc converter structure, and the fluctuating amplitude of the dc input current of the high-frequency inverter is greatly declined. However, as the number of parallel modules of the dc–dc converter is increased, the maximum peak-to-peak value of the output current is not significantly improved, and the occurrence frequency of the maximum peak-to-peak value of the output current is greatly reduced.

2) Simulation Scheme 2: To verify the superiority of the proposed control method in this article in reducing the dc output current ripple of the odd number of dc–dc converter modules connected in parallel, Fig. 6 shows the simulation results of the odd number of dc–dc converter modules based electrolysis power supply using different control methods. Fig. 6(a) shows the simulation result when a conventional control method is used for the electrolysis power supply based on multiple dc–dc converter modules connected in parallel. Fig. 6(b) shows the simulation result when the proposed control method in this article is used for the electrolysis power supply based on multiple dc–dc converter modules connected in parallel. Fig. 6(c) shows the frequency spectrum diagram of the current components of each

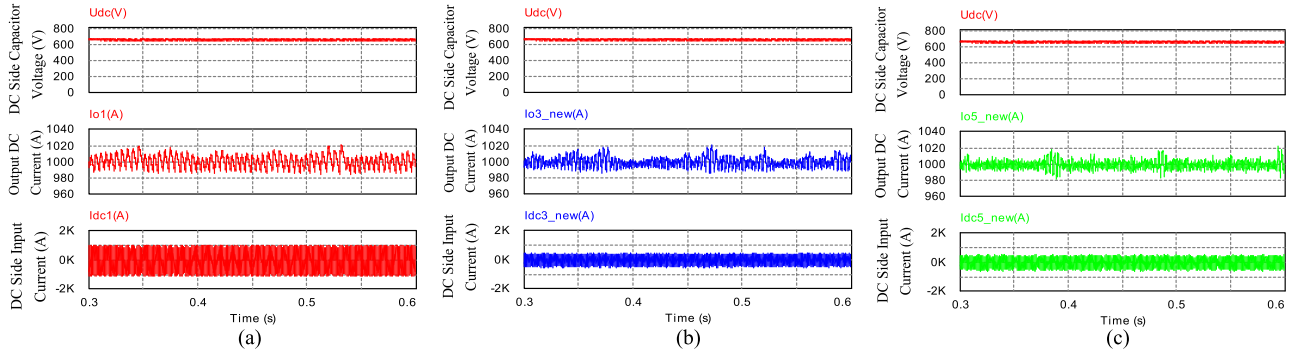

Fig. 5. Simulation results of dc–dc converters with different topologies. (a) Simulation result of the electrolysis power supply with single dc–dc converter module. (b) Simulation results of the electrolysis power supply based on the parallel configuration with three dc–dc converter modules. (c) Simulation results of the electrolysis power supply based on the parallel configuration with five dc–dc converter modules.

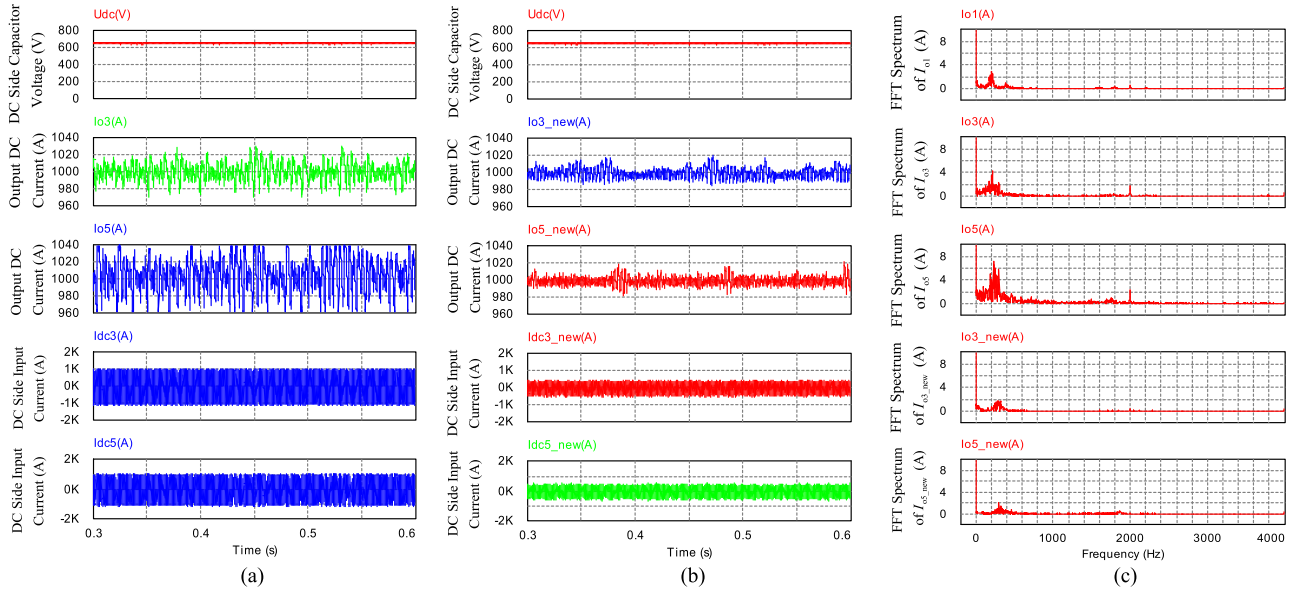

Fig. 6. Simulation results of dc–dc converters with different control methods. (a) Simulation results of the electrolysis power supply with the conventional control method. (b) Simulation results of the electrolysis power supply with the proposed control method. (c) Frequency spectrums of the output current when the electrolysis power supply was controlled by the conventional control method and the proposed control method respectively.

frequency in the dc output current, wherein the magnitude of the dc component is 1000 A. In Fig. 6, $U_{\rm dc}$ is the dc-side capacitor voltage of the front-stage PWM rectifier. $I_{\rm o3}$ is the dc output current of the electrolysis power supply when the same control method is used for the three dc–dc converter parallel modules. $I_{\rm o3-new}$ is the dc output current of the electrolysis power supply when the control method proposed in this article is used for the three dc–dc converter parallel modules. $I_{\rm o5}$ is the dc output current of the electrolysis power supply when the same control method is used for the five dc–dc converter parallel modules. $I_{\rm o5-new}$ is the dc output current of the electrolysis power supply when the control method proposed in this article is used for the five dc–dc converter parallel modules. $I_{\rm dc3}$ is the dc-side input current of the high-frequency inverter when the same control method is used for the three dc–dc converter parallel modules. $I_{\rm dc3-new}$ is the dc input current of the high-frequency inverter when the three dc–dc converter parallel modules are controlled by the control method proposed in this article. $I_{\rm dc5}$ is the dc input current of the high-frequency inverter when the same control method is used for the five dc–dc converter parallel modules. $I_{\rm dc5-new}$ is the dc input current of the high-frequency inverter when the five dc–dc converter modules are controlled by the control method proposed in this article.

From Fig. 6(a) and (b), we can see that the peak-to-peak value of the output current of the electrolysis power supply adopting the control method proposed in this article is greatly reduced compared with the traditional control method. At the same time, the fluctuating amplitude of the dc input current of the high-frequency inverter is also greatly reduced. From Fig. 6(c), we can see that the harmonic content in the dc output current is reduced when the electrolysis power supply adopting the proposed control method.

3) Simulation Scheme 3: In order to further verify the applicability of the proposed topology and control method, the simulation effect of dc output current when the number of parallel dc–dc converters is more than five is shown in Fig. 7(a). To

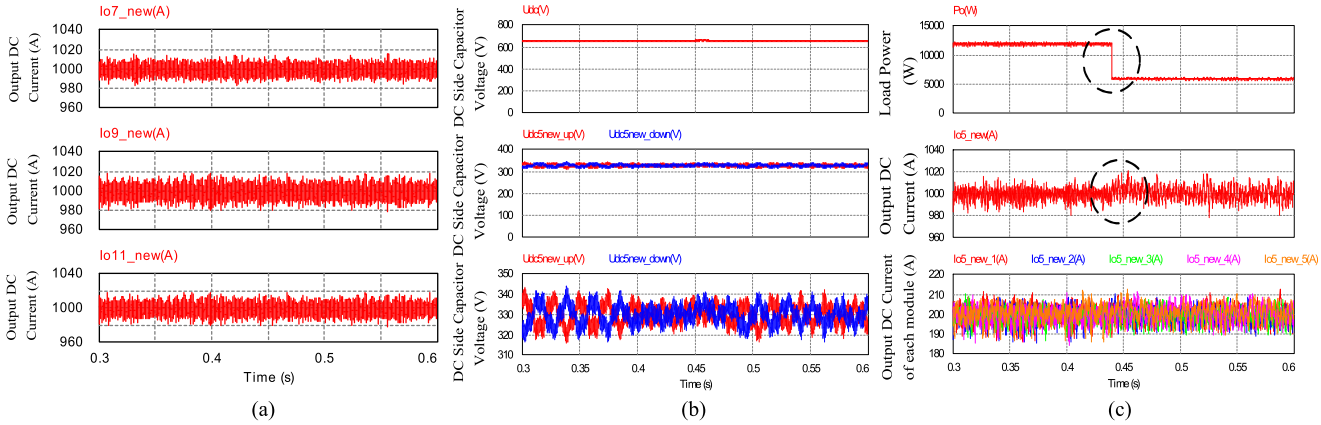

Fig. 7. Simulation results of the dynamic performance of the electrolysis power supply adopted the proposed topology and control method. (a) Output current of the electrolysis power supply when the number of parallel dc–dc converters is more than five. (b) Capacitor voltage of the upper and lower arms of the split dc-link with series cap. (c) Output current of each dc–dc conversion module connected in parallel when the load is suddenly reduced by 50%.

verify the validity of the proposed control method in balancing the output current of each dc–dc conversion module connected in parallel and load transient performance, Fig. 7(b) shows the capacitor voltage of the upper and lower arms of the split dc-link with series cap, and Fig. 7(c) shows the output current of each dc–dc conversion module connected in parallel when the load is suddenly reduced by 50%. In Fig. 7(a), $I_{\mathrm{o7-new}}$, $I_{\mathrm{o9-new}}$, and $I_{\mathrm{o11-new}}$ are the dc output current of the electrolysis power supply when the proposed control method is applied to the 3, 7, and 11 dc–dc converter parallel modules, respectively. In Fig. 7(b), $U_{\mathrm{dc5new\_up}}$ and $U_{\mathrm{dc5new\_down}}$ are the capacitor voltages of the upper and lower arms of the split dc-link with series cap, respectively. In Fig. 7(c), P_{o} is the output power of the electrolysis power supply, and $I_{\mathrm{o5-new-1}}$, $I_{\mathrm{o5-new-2}}$, $I_{\mathrm{o5-new-3}}$, $I_{\mathrm{o5-new-4}}$, and $I_{\mathrm{o5-new-5}}$ are the output currents of five parallel modules, respectively.

From Fig. 7(a), it can be seen that the dc output current ripple of the proposed electrolysis power supply is small when the number of the parallel connected dc–dc becomes greater than five. However, the amplitude of the maximum peak-to-peak value of the output current does not drop significantly as the number of parallel-connected dc–dc converter modules increase. From Fig. 7(b), it can be seen that the maximum deviation of the capacitor voltages of the upper and lower arms of the split dc-link with series cap from the reference voltage is 3.5%. From Fig. 7(c), it can be seen that the output current $(I_{\mathrm{o5-new}})$ of the electrolytic power source adopting the proposed topology and control method has good constant current characteristics when the power (P_{o}) of the load is suddenly decreased from 12 to 6 kW. At the same time, each parallel module in the power supply has a good current-sharing capability.

B. Experiment

Considering the cost and volume, the prestage three-phase PWM rectifier circuit in this article is designed as a whole, and each poststage dc–dc module, as shown in Fig. 8, is designed as a whole. The input end and output end of dc–dc can be connected in parallel to construct a large current power supply. The rated

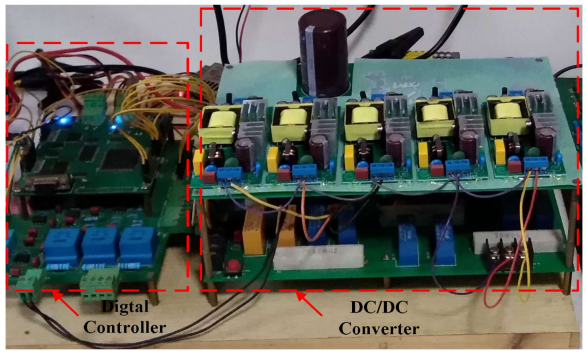

Fig. 8. Experimental setup of the electrolysis power supply.

output current of the poststage dc–dc converter is 20 A, and 0.4-Ω resistor is used for the load of the electrolysis power supply. The poststage dc–dc converter of electrolysis power supply consists of five dc–dc converter modules connected in parallel. The power switching devices of three-phase PWM rectifier and high-frequency inverter are IGBT (FGL40N120) and MOSFETs (2SK3569), respectively. The controller of electrolysis power supply is based on TMS320F2812. The rest parameters of the electrolysis power supply are shown in Table II, and the experimental setup of electrolysis power supply is shown in Fig. 8.

Fig. 9 shows the output current waveform of the electrolysis power supply adopted different topology and control method. Fig. 9(a) shows the dc output current waveform of a single dc–dc converter, and the maximum peak-to-peak value of the dc output current is about 1.21 A. Fig. 9(b) shows the dc output current waveform of the electrolysis power supply when the same control method is used for the five dc–dc converter parallel modules, and the maximum peak-to-peak value of the dc output current is about 2.23 A. Fig. 9(c) shows the dc output current waveform of the electrolysis power supply when the control method proposed in this article is used for the five dc–dc converter parallel modules. Except for the occasional peak-to-peak value of 1.2 A, the peak value of the output current is about 0.59 A at other time periods.

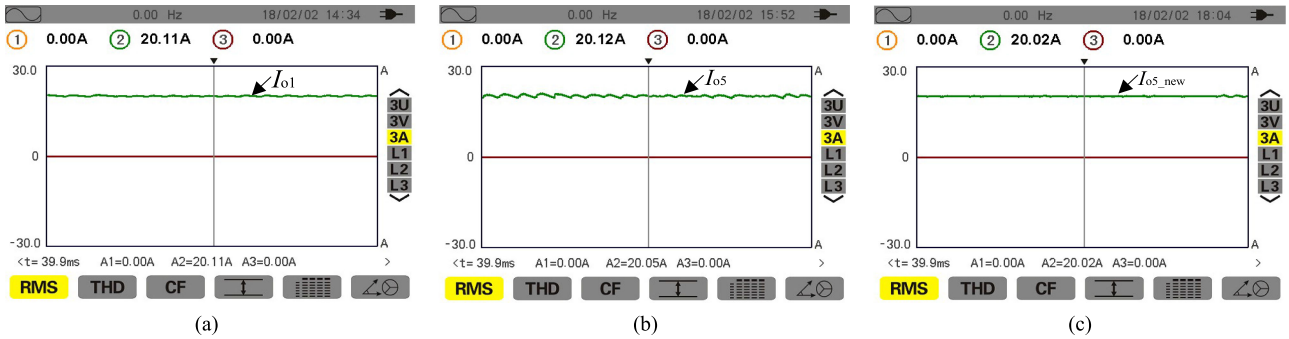

Fig. 9. Output current waveforms of electrolysis power supply with different topologies and control methods. (a) Output current of the electrolysis power supply with single dc–dc converter module. (b) Output current of the electrolysis power supply when the same control method is used in the five parallel dc–dc converter modules. (c) Output current of the electrolysis power supply when the proposed control method is used in the five parallel dc–dc converter modules.

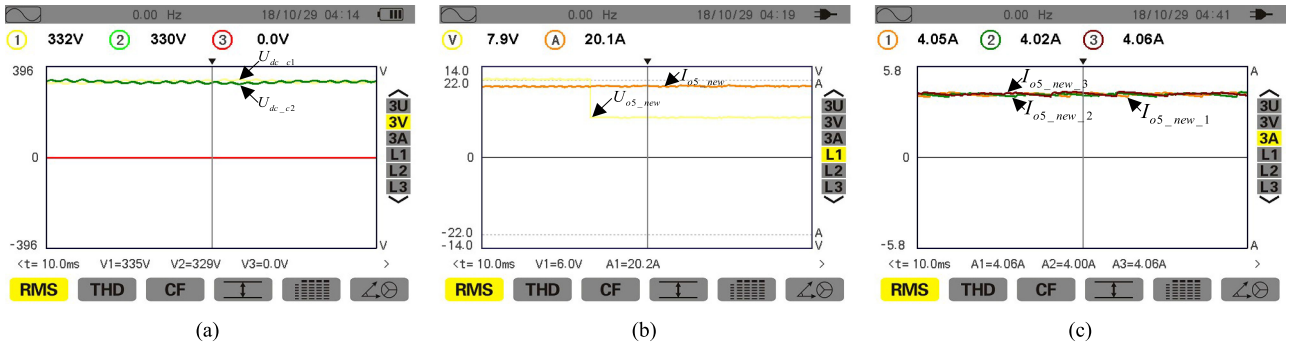

Fig. 10. Dynamic performance of the converters adopted the proposed topology and control method. (a) Capacitor voltage of the upper and lower arms of the split dc-link with series cap. (b) Output voltage and current of the electrolysis power supply with five parallel dc–dc converter modules when the load is suddenly reduced by 50%. (c) Output current of each dc–dc conversion module connected in parallel when the load is suddenly reduced by 50%.

From Fig. 9, it can be seen that the topology and control method of electrolysis power supply proposed in this article can effectively improve the current ripple characteristics of the output current of the electrolysis power supply, and the occurrence frequency of the maximum peak-to-peak value in the dc output current of the electrolysis power supply greatly decreases as the number of parallel-connected dc–dc converter modules increases.

Fig. 10 shows the dynamic performance of converters using the proposed topology and control method. Fig. 10(a) shows the capacitor voltage of the upper and lower arms of the split dc-link with series cap. Fig. 10(b) shows the output current of each dc–dc conversion module connected in parallel when the load is suddenly reduced by 50%. Fig. 10(c) shows the output current of each dc–dc conversion module connected in parallel when the load is suddenly reduced by 50%. In Fig. 10(a), $U_{\mathrm{dc-c1}}$ and $U_{\mathrm{dc-c2}}$ are the capacitor voltages of the upper and lower arms of the split dc-link with series cap, respectively. In Fig. 10(b), $U_{\mathrm{o5-new}}$ and $I_{\mathrm{o5-new}}$ are the dc output voltage of the electrolysis power supply, respectively. In Fig. 10(c), $I_{\mathrm{o5-new-1}}$, $I_{\mathrm{o5-new-2}}$, and $I_{\mathrm{o5-new-3}}$ are the output currents of the first, second, and third dc–dc modules, respectively.

From Fig. 10, it can be seen that the output current $(I_{\mathrm{o5-new}})$ of the electrolytic power source adopting the proposed topology and control method has good constant current characteristics and good current-sharing capability.

TABLE III
EFFICIENCY OF POWER SUPPLY AT DIFFERENT POWER LEVELS

Parameters	Value			
Power rate of power supply	100W	150W	200W	250W
Efficiency of power supply	0.846	0.877	0.889	0.888

The efficiency of power supply at different power levels is shown in Table III. According to the efficiency standards (see Table I) shown in [18] and Table III, it can be seen that the efficiency of the proposed power supply is acceptable in current electrolysis power supply.

V. CONCLUSION

This article proposes a multiphase high-frequency inverter based electrolysis power supply topology and phase equalization staggered control method; the lower harmonic components of the output current of each dc–dc conversion module cancel each other, thereby reducing the ripple component in the total output current of the electrolysis power supply. Simulation and experimental results show that the proposed topology and control method of electrolysis power supply can effectively improve the ripple characteristics of the dc output current of electrolysis power supply. The main features of the propose electrolysis power supply are as follows.

1) Compared with the structure of a single dc–dc converter, the proposed topology and control method can greatly reduce the occurrence frequency of the maximum peak-to-peak value of the dc output current of the electrolysis power supply.
2) Compared with the traditional control method used in the parallel structure of multiple dc–dc conversion modules, the proposed control method can greatly reduce the maximum peak-to-peak value of the dc output current of the electrolysis power supply, and can also reduce the occurrence frequency of the maximum peak-to-peak value in the dc output current of the electrolysis power supply.
3) Since the high harmonic contents in the dc output current of the electrolysis power supply are less and are easily filtered out by the *LC* filter, the improvement effect of the proposed method on the current ripple characteristics of electrolysis power supply is weaker with the number of dc–dc conversion modules connected in parallel increasing when the number of dc–dc conversion modules connected in parallel is large.

ACKNOWLEDGMENT

The author would like to thank all editors and reviewers for their continuous encouragement and support.

REFERENCES

[1] Y. Gu and D. Zhang, "Interleaved boost converter with ripple cancellation," *IEEE Trans. Power Electron.*, vol. 28, no. 8, pp. 3860–3869, Aug. 2013.
[2] J. Solanki, N. Fröhleke, J. Böcker1, A. Averberg, and P. Wallmeier, "High-current variable-voltage rectifiers: State of the art topologies," *IET Power Electron*., vol. 8, no. 6, pp. 1068–1080, 2015.
[3] X. Tan and X. Ruan, "Optimal design of DCM LCC resonant converter with inductive filter based on mode boundary map," *IEEE Trans. Power Electron.*, vol. 30, no. 8, pp. 4144–4155, Aug. 2015.
[4] B. Sarrazin, R. Hanna, and P. Lefranc, "Insulated power supply for gate drivers up to 40 kV for medium-voltage direct current applications," *IET Power Electron.*, vol. 10, no. 15, pp. 2143–2148, 2017.
[5] N. Mohan *et al.*, *Power Electronics: Converters Applications and Design*, 3rd ed. New York, NY, USA: Wiley, 2003.
[6] Y. Tang, Z. Qin, F. Blaabjerg, and P. Loh, "A dual voltage control strategy for single-phase PWM converters with power decoupling function," *IEEE Trans. Power Electron.*, vol. 30, no. 12, pp. 7060–7071, Dec. 2015.
[7] Y. Yang, X. Ruan, L. Zhang, J. He, and Z. Ye, "A feed-forward scheme for an electrolytic capacitor-less ac/dc LED driver to reduce output current ripple," *IEEE Trans. Power Electron.*, vol. 29, no. 10, pp. 5508–5517, Oct. 2014.
[8] H. Li, Y. Zhang, and C. Zhang, "A repetitive inductive pulsed power supply circuit topology based on HTSPPT," *IEEE Trans. Plasma Sci.*, vol. 46, no. 1, pp. 134–139, Jan. 2018.
[9] D. G. Bandeira, Jr., T. B. Lazzarin, and I. Barbi, "High voltage power supply using T-type parallel resonant DC-DC converter," *IEEE Trans. Ind. Appl.*, vol. 54, no. 3, pp. 2459–2470, May/Jun. 2018.
[10] X. Huang, X. Ruan, and F. Du, "A pulsed power supply adopting active capacitor converter for low-voltage and low-frequency pulsed load," *IEEE Trans. Power Electron.*, vol. 33, no. 11, pp. 9219–9230, Nov. 2018.
[11] P. Buddingh and J. S. Mars, "New life for old thyristor power rectifiers using contemporary digital control," *IEEE Trans. Ind. Appl.*, vol. 36, no. 5, pp. 1449–1454, Sep./Oct. 2000.
[12] R. Kalpana, G. Bhuvaneswari, B. Singh, and S. Singh, "Harmonic mitigator based on 12-pulse ac–dc converter for switched mode power supply," *IET Power Electron*., vol. 3, no. 6, pp. 947–964, Nov. 2010.
[13] A. P. Agalgaonkar, K. M. Muttaqi, and S. Perera, "Open loop response characterization of an aluminum smelting plant for short time interval feeding," in *Proc. IEEE Power Energy Soc. Gen. Meeting*, 2009, pp. 26–30.
[14] J. Solanki, N. Frohleke, J. Bocker, and P. Wallmeier, "A modular multilevel converter based high-power high-current power supply," in *Proc. IEEE Int. Conf. Ind. Technol.*, 2013, pp. 444–450.
[15] S. A. Saleh, B. Allen, and E. Ozkop, "Multistage and multilevel power electronic converter-based power supply for plasma DBD devices," *IEEE Trans. Ind. Electron.*, vol. 65, no. 7, pp. 5466–5475, Jul. 2018.
[16] Z. M. Shafik, M. I. Masoud, J. E. Fletcher, S. J. Finney, and B. W. Williams, "Efficiency improvement techniques of high current low voltage rectifiers using MOSFETs," in *Proc. 44th Int. Univ. Power Eng. Conf.*, 2010, pp. 1–7.
[17] E. Coulinge, J.-P. Burnet, and D. Dujic, "High-current low-voltage power supplies for superconducting magnets," in *Proc. 19th Int. Symp. Power Electron.*, Oct. 2017, pp. 1–6.
[18] J. Aguillon-Garcia and G.-W. Moon, "A high-efficiency three-phase ZVS PWM converter utilizing a positive double-star active rectifier stage for server power supply," *IEEE Trans. Ind. Electron.*, vol. 58, no. 8, pp. 3317–3329, Aug. 2011.
[19] J. I. Guzman, C. R. Baier, J. R. Espinoza, P. E. Melin, and J. A. Munoz, "Comparison of CSI and VSI based modular rectifiers with magnetic AC coupling for large current and low voltage applications," in *Proc. 38th Annu. Conf. IEEE Ind. Electron. Soc.*, 2012, pp. 293–298.
[20] P. C. Heris, Z. Saadatizadeh, and E. Babaei, "A new two input-single output high voltage gain converter with ripple-free input currents and reduced voltage on semiconductors," *IEEE Trans. Power Electron.*, vol. 34, no. 8, pp. 7693–7702, Aug. 2019.
[21] Z. Li, R. Lizana, and S. M. Lukic, "Current injection methods for ripple-current suppression in delta-configured split-battery energy storage," *IEEE Trans. Power Electron.*, vol. 34, no. 8, pp. 7411–7421, Aug. 2019.
[22] J. G. Kassadian, F. S. Marton, and G. C. Verghese, *Principle of Power Electronics*. Reading, TX, US: Addison-Wedey, 1991.
[23] H. Xiao, A. Luo, Z. Shuai, G. Jin, and Y. Huang, "An improved control method for multiple bidirectional power converters in hybrid AC/DC microgrid," *IEEE Trans. Smart Grid*, vol. 7, no. 1, pp. 340–347, Jan. 2016.
[24] A. Luo, H. Xiao, and Z. Shuai, "Double deadbeat-loop control method for distribution static compensator," *IET Power Electron.*, vol. 8, no. 7, pp. 1104–1110, 2015.

Huagen Xiao received the Ph.D. degree from Hunan University, Changsha, China, in 2015.

From 2005 to 2008, he was an Engineer with Zhuhai Power Station, Zhuhai, China. Since 2017, he has been an Associate Professor with the Hunan University of Science and Technology, Xiangtan, China. His research interests include power conversion systems.